Supporting Information: Genuine dynamics vs cross phase modulation artefacts in Femtosecond Stimulated Raman Spectroscopy

Giovanni Batignani,[†] Giuseppe Fumero,[†,‡] Emanuele Pontecorvo,[†] Carino Ferrante,[†,¶] Shaul Mukamel,[§] and Tullio Scopigno*[,†,¶]

†*Dipartimento di Fisica, Universitá di Roma "La Sapienza", Roma, I-00185, Italy*

‡*Dipartimento di Scienze di Base e Applicate per l'Ingegneria, Universitá di Roma "La Sapienza", I-00185, Roma, Italy*

¶ *Istituto Italiano di Tecnologia, Center for Life Nano Science @Sapienza, Roma, I-00161, Italy*

§*Department of Chemistry, University of California, Irvine, California 92697-2025 (USA).*

E-mail: tullio.scopigno@phys.uniroma1.it

- In Table S1 we report the system parameters, extracted from the fit procedure reported in Fig. 1 of the manuscript.

- In Fig. S1 we report the slices, for selected time delays, of the colormap shown in Fig.1 of the manuscript.

- In Fig. S2, we report the AP_{Off} and AP_{On} FSRS spectra (blue dots and black lines, respectively), compared with the reconstructed FSRS spectrum (red lines), obtained

subtracting from the AP_{On} spectra the calculated XPM artefact. FSRS experimental spectra correspond to differential traces reported in Fig. 4 of the manuscript.

- In Fig. S3, we report the spectral and temporal dependence of the differential FSRS spectra on linear and quadratic dispersion terms (β_1 and β_2, respectively) for negative time delays ($T = -2$ ps and $T = -1$ ps).

- In Fig. S4, we report the spectral and temporal dependence of the differential FSRS spectra on linear and quadratic dispersion terms (β_1 and β_2, respectively) around $T = 0$.

- In Figs. S5 and S6 the stimulated Raman gain and differential FSRS spectral dependence on the RP intensity is reported.

- In Fig. S7 the differential FSRS spectral dependence (evaluated as maximum of the $\Delta FSRS$ signal and as peak shift) on the AP intensity is reported.

- In Fig. S8 the XPM artefact spectral dependence as a function of the sample thickness is reported, showing that it grows linearly with (small) L.

Table S1: Sample fit parameters used for Fig. 1: $\tilde{\nu}$ indicates the peak position, A the relative amplitude and Γ the linewidth.

$\tilde{\nu}$ (cm^{-1})	A (AU)	Γ (cm^{-1})
801.7	5.47	3.1
1028.6	3.28	13.4
1157.8	0.43	3.3
1266.8	2.91	12.7
1443.9	3.25	14.8
1465.2	0.19	7.0

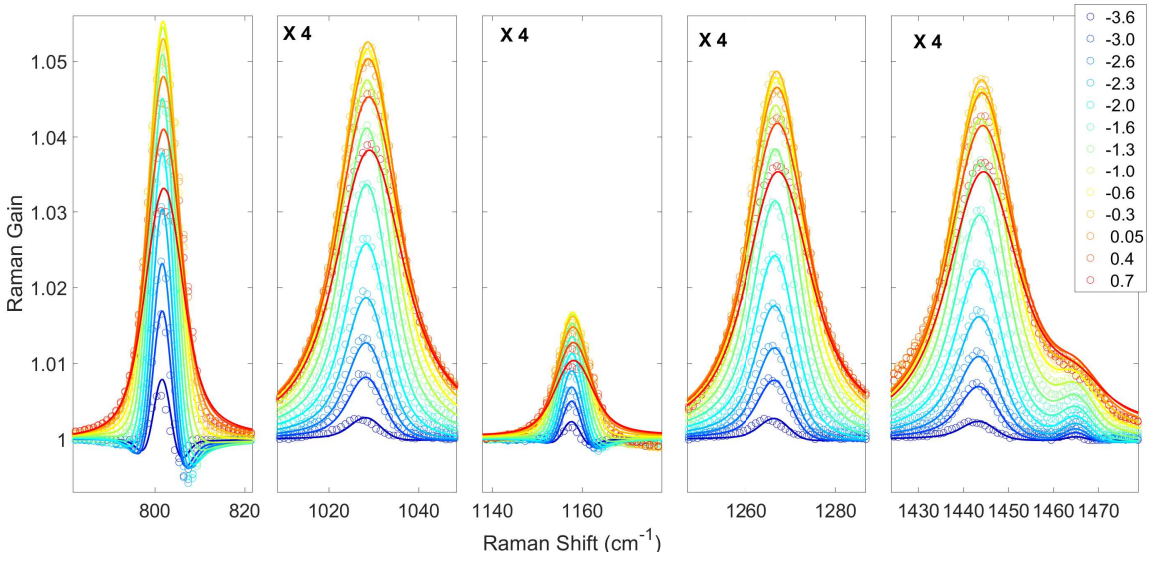

Fig. S1: **Broadband stimulated Raman spectra of liquid Cyclohexane**: Slices of Fig.1, for selected time delays (reported in the legend in picoseconds). Experimental spectra of the non-resonant SRS spectrum, shown as dots, are compared with the simulated ones (lines). Six vibrational modes (at 801, 1028, 1158, 1266, 1444, 1465 cm^{-1}) are monitored in order to calibrate the experimental parameters for the FSRS experiment. Beyond 900 cm^{-1} the data have been 4X scaled.

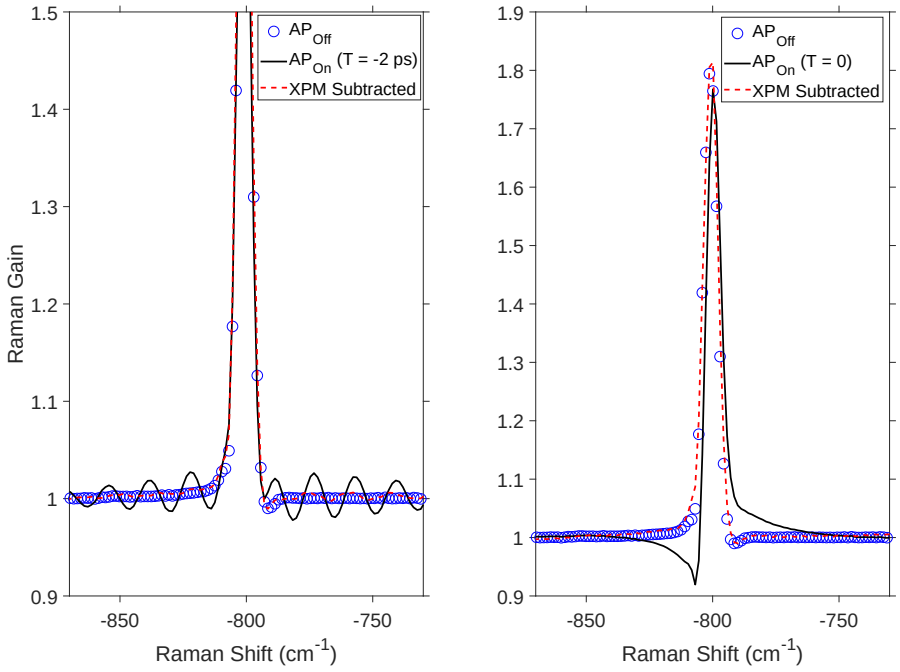

Fig. S2: **Retrieval of the genuine FSRS response, by subtracting the modelled XPM artefacts**: Experimental FSRS spectra measured without AP (blue dots) are compared with the experimental FSRS spectra measured with AP excitation, hence affected by XPM artefacts (black lines), and the reconstructed FSRS spectrum, obtained subtracting from the AP_{On} spectra the calculated XPM artefact (red lines), for T = -2 ps and T = 0 ps (the relative time delay between PP and RP is ΔT_{R-P} = 0.9 ps). The corresponding differential FSRS spectra measured with and without AP are reported in Fig. 4 of the manuscript.

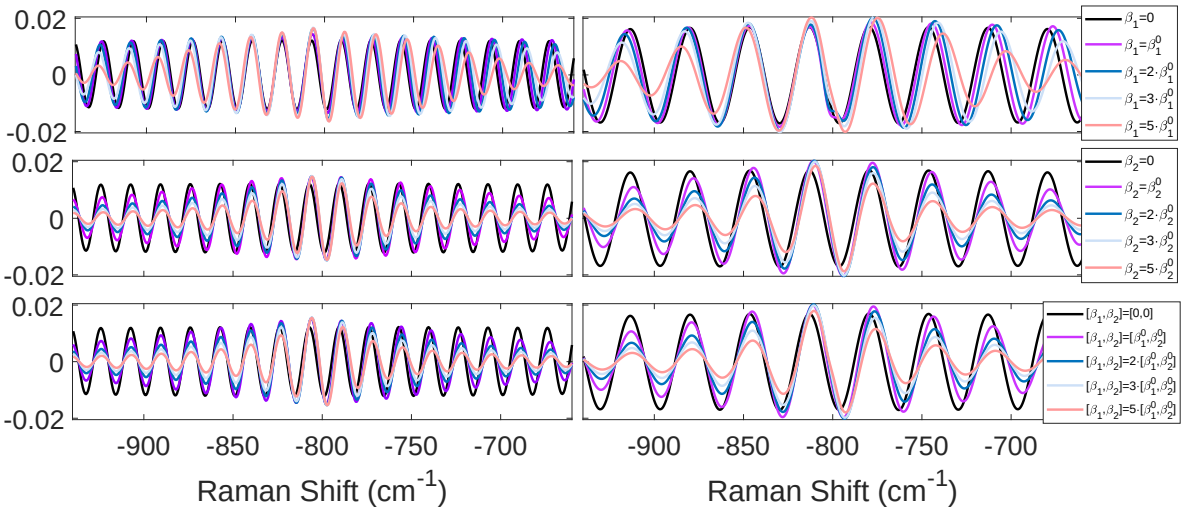

Fig. S3: **Differential Raman gain spectra dependence on dispersion**: Simulated differential Raman gain spectra for a 800 cm^{-1} Raman mode (3.1 cm^{-1} linewidth) for negative time delays between AP and PP (T = -2 ps in the left panel and T = -1 ps in the right one). The linear and quadratic dispersion parameters (β_1^0 and β_2^0) correspond to the Cyclohexane one, and the XPM artefacts are evaluated propagating the beams in a 5 mm sample, in order to emphasize the effect. As can be seen the spectral width of the oscillations in the ΔFSRS spectra is reduced as the dispersion is increased. In fact, the spectral width of such features is inversely proportional to the AP time duration, and the presence of large β_2 increases the effective AP time duration along the sample pathlength. The presence of β_1 generates a temporal delay T between AP and PP, which is different at different position (z) across the sample, due to the different group velocities of the two beams: since the period of the oscillations is inversely proportional to T, the total signal originates from components oscillating with different periods, which hence will be in phase around the 800 cm^{-1} peak position and out of phase away from it, resulting in a decrease of the oscillating feature spectral width.

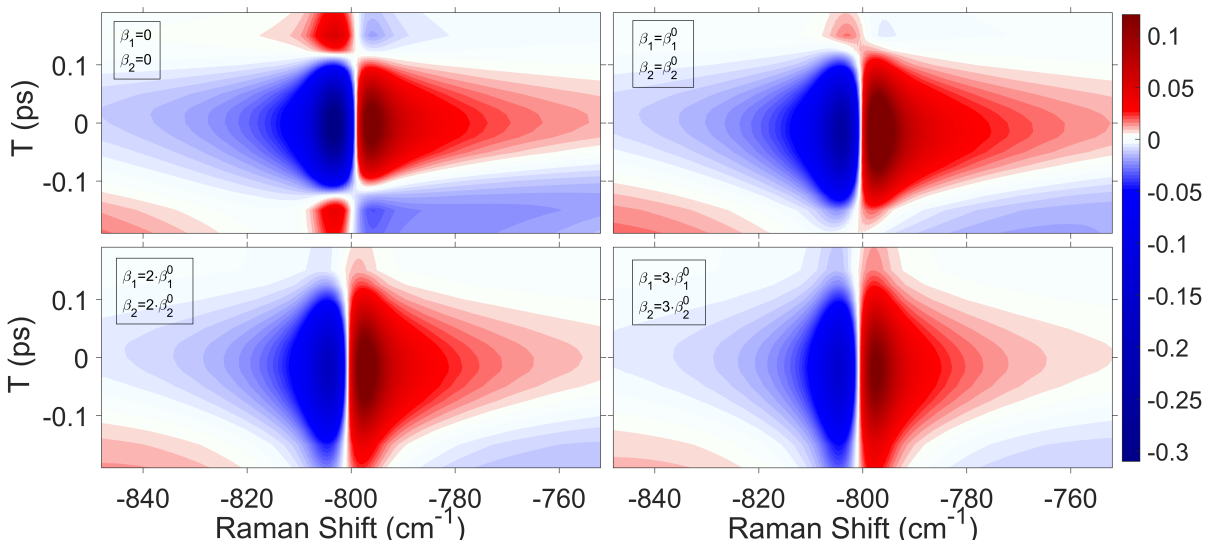

Fig. S4: **Differential Raman gain spectra dependence on dispersion**: Simulated differential Raman gain spectra for a 800 cm^{-1} Raman mode (3.1 cm^{-1} linewidth) as a function of AP-PP relative time delay, for $\Delta T_{R-P} = 0$. The linear and quadratic dispersion parameters (β_1^0 and β_2^0) correspond to the Cyclohexane one, and the XPM artefacts are evaluated propagating the beams in a 5 mm sample, in order to emphasize the effect. As can be seen, an increased dispersion results in a broadening of the temporal width of the XPM artefact, in view of the increase of the AP temporal duration.

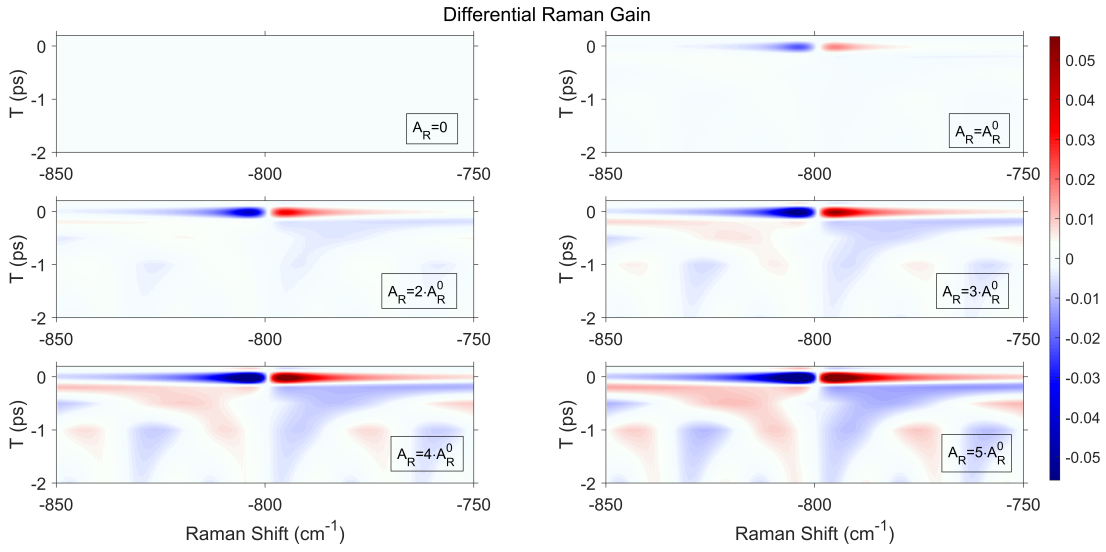

Fig. S5: **Differential Raman gain spectra dependence on the RP intensity**: Differential Raman gain spectra are simulated for equally spaced different RP intensities, for a 800 cm^{-1} Raman mode (3.1 cm^{-1} linewidth) as a function of AP-PP relative time delay. The simulation has been performed considering $\Delta T_{R-P} = 0$, $\beta_1 = 0$ and $\beta_2 = 0$.

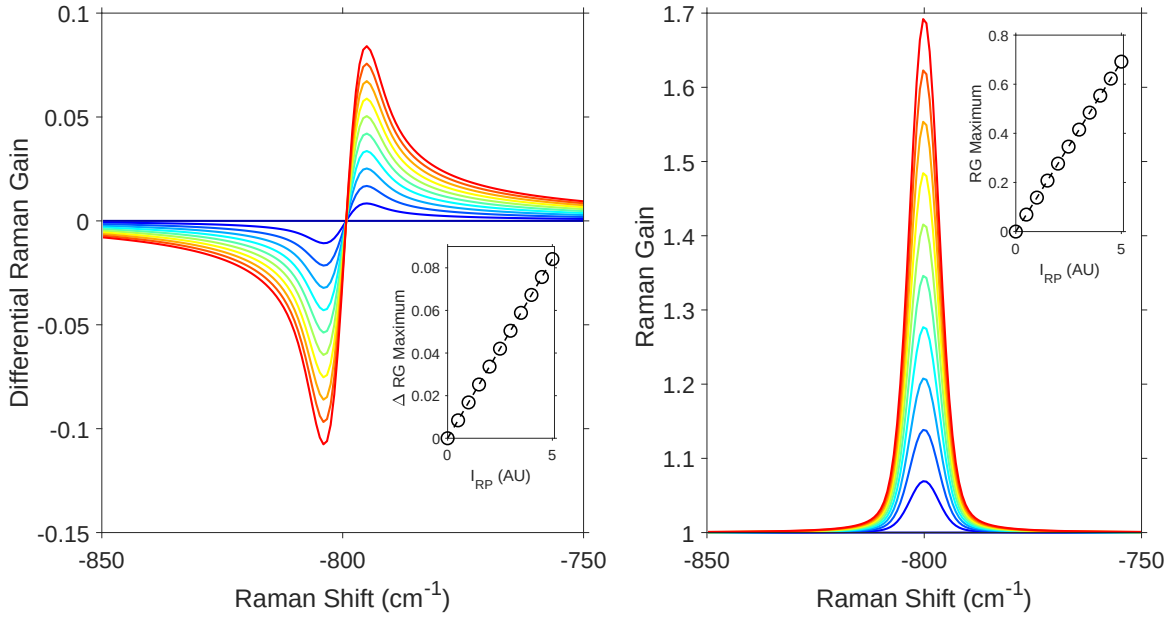

Fig. S6: **ΔFSRS and SRS spectral dependence on the RP intensity**. The spectral dependence of the differential Raman Gain is reported in the left panel, while the stimulated Raman spectrum is reported in the right ones. The spectra are simulated for equally spaced different RP intensities, for a 800 cm^{-1} Raman mode (3.1 cm^{-1} linewidth). In the simulation we set $\Delta T_{R-P} = 0$, $\beta_1 = 0$ and $\beta_2 = 0$. In the inset we report (as black dots) the maximum amplitude of Δ FSRS and SRS signal, which indicates a linear dependence of both the signals on the RP intensity.

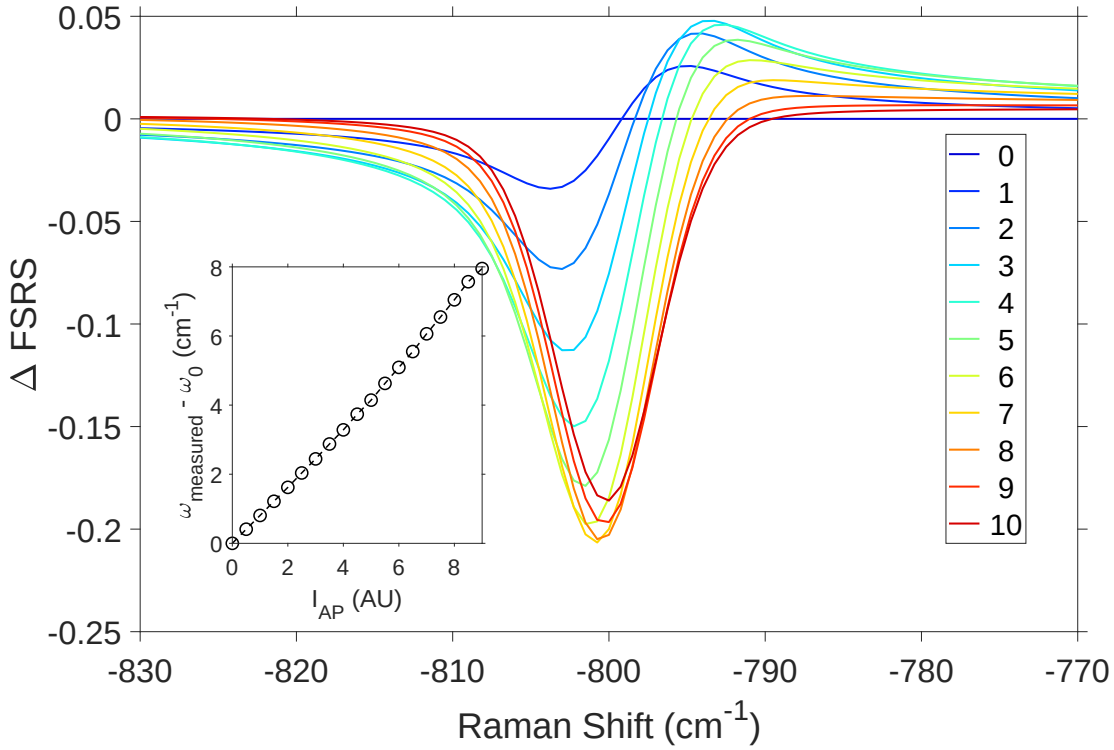

Fig. S7: **ΔFSRS spectral dependence on the AP intensity**. The spectra are simulated for equally spaced different AP intensities, for a 800 cm^{-1} Raman mode (3.1 cm^{-1} linewidth). In the simulation we set $\Delta T_{R-P} = 0$, $\beta_1 = 0$ and $\beta_2 = 0$. In the inset we report the apparent peak shift of the Raman mode, evaluated as the peak position measured in presence and in absence of the XPM artefact, which shows a linear dependence on the AP intensity.

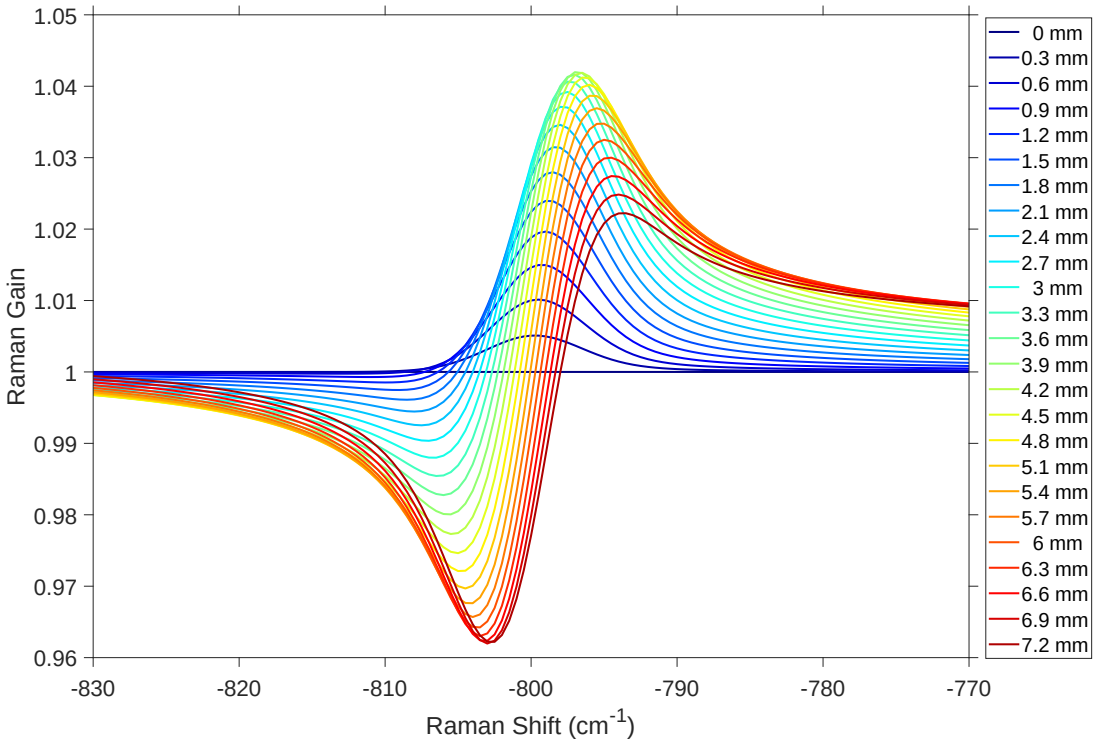

Fig. S8: **ΔFSRS spectral dependence on the effective pathlength** L. The spectra are simulated for equally spaced different sample path L, for a 800 cm^{-1} Raman mode (3.1 cm^{-1} linewidth). In the simulation we set $\Delta T_{R-P} = 0$, $\beta_1 = 0$ and $\beta_2 = 0$.